Crystal structure of human carbonic anhydrase II complexed with an anti-convulsant sugar sulphamate

Rosario RECACHA*, Michael J. COSTANZO†, Bruce E. MARYANOFF† and Debasish CHATTOPADHYAY*[1]

*Center for Biophysical Sciences and Engineering, and School of Medicine, University of Alabama at Birmingham, Birmingham, AL 35294, U.S.A., and †The R. W. Johnson Pharmaceutical Research Institute, Spring House, PA 19477, U.S.A.

The fructose-based sugar sulphamate RWJ-37497, a potent analogue of the widely used anti-epileptic drug topiramate, possesses anti-convulsant and carbonic anhydrase-inhibitory activities. We have studied the binding interactions of RWJ-37497 in the active site of human carbonic anhydrase II by X-ray crystallography. The atomic positions of the enzyme inhibitor complex were refined at a resolution of 2.1 Å (1 Å = 0.1 nm) to the final crystallographic R and R_{free} values of 0.18 and 0.23, respectively. The inhibitor co-ordinates to the active-site zinc ion through its oxygen atom and the ionized nitrogen atom of the sulphamate group by replacing the metal-bound water molecules, although the sulphamoyl oxygen atom provides a rather lengthy co-ordination. The 4,5-cyclic sulphate group is positioned in a hydrophobic pocket of the active site, making contacts with the residues Phe-131, Leu-198, Pro-201 and Pro-202. Since the ligand was found to be intact, concerns about RWJ-37947 irreversibly alkylating the enzyme through its 4,5-cyclic sulphate group were dispelled.

Key words: drug design, epilepsy, glaucoma, protein structure, topiramate.

INTRODUCTION

Carbonic anhydrase (CA; EC 4.2.1.1) is a zinc-containing enzyme [1,2] that catalyses the reversible hydration of carbon dioxide: $CO_2 + H_2O \leftrightarrow HCO_3^- + H^+$. This reaction is essential for important physiological anion-exchange processes [3], and the enzyme is the target of drugs for the treatment of glaucoma. Inhibition of the synthesis of HCO_3^- from CO_2 and OH^- reduces aqueous humour formation and lowers intra-ocular pressure, which is the major risk factor for primary open-angle glaucoma [4,5].

There are three evolutionarily unrelated CA families, designated α, β and γ, with no significant sequence homology. Seven genetically distinct mammalian CA α isoenzymes with different tissue distributions and intracellular locations, CAs I–VII, have been identified. There are also some important differences among these isoenzymes with respect to their catalytic efficiencies and inhibitor-binding properties [6]. CA II, the most studied form, has an exceptionally high CO_2 hydration rate and a wide tissue distribution. Human CA (HCA) II comprises a single polypeptide chain with a molecular mass of 29.3 kDa. The enzyme contains one catalytic zinc ion, co-ordinated to three histidine residues, His-94, His-96 and His-119. A tetrahedral co-ordination sphere is completed with a water molecule, which forms a hydroxide ion with a pK_a value of 7.0.

The inhibitor of interest, RWJ-37947 (see Figure 1a), possesses a sugar sulphamate structure that is derived from the natural monosaccharide D-fructose and is a potent analogue of the widely used anti-epileptic drug topiramate (Figure 1a) [7]. RWJ-37947 exhibits potent anti-convulsant activity in mice and rats as determined by the standard maximal electroshock seizure (MES) test [7]. This compound is chemically related to sulphonamides in that it bears an SO_2NH_2 functional group, which is recognized as important in the aryl and heteroaryl sulphonamide classes of CA inhibitors by virtue of co-ordination to the zinc atom in the enzyme's active site. Since compounds of this type can have many useful applications, for example as diuretic, anti-glaucoma or anti-epileptic drugs [8], they constitute an important class of biologically active agents. Thus knowledge of the interactions between sulphonamide-type inhibitors and HCA is of pharmacological and therapeutic interest for understanding their mechanism of inhibition and for the design of better drugs.

RWJ-37947 has an unusual structure for a potent CA inhibitor, as it does not contain a planar arene or heteroarene group and is sterically globular. It inhibits the rat myelin enzyme, which is comprised mainly of CA II, and the human erythrocyte enzyme, which is comprised of CA I and CA II [7,9]. The IC_{50} values of RWJ-37947 for rat myelin CA II and purified human erythrocyte CA II are 52 and 36 nM, respectively (R. Shank and B. E. Maryanoff, unpublished work). The corresponding IC_{50} values for topiramate are 1.4 and 1.5 μM, respectively [9]. Since analysis of its binding to the enzyme could reveal new modes of interaction with the enzyme, we determined the crystal structure of HCA II complexed with RWJ-37947 to a resolution of 2.1 Å (1 Å = 0.1 nm). RWJ-37947 is clearly resolved in the active site of the enzyme and binds to the metal ion as an anion, $R\text{-}SO_2NH^-$, via the nitrogen atom and an oxygen atom of the sulphamate group. Additionally, RWJ-37947 interacts with a hydrophobic pocket within the active site.

EXPERIMENTAL

Crystallization

Purified recombinant HCA was kindly supplied by Professor J. Beckman at the University of Alabama at Birmingham, Birmingham, AL, U.S.A. RWJ-37947 was added in a 2-fold molar excess to the protein (5 mg/ml) with 4 mM dithiothreitol, which served to prevent formation of intermolecular disulphide bridges. Crystals were obtained by the hanging-drop vapour-diffusion method at 4 °C using 2.8 M $(NH_4)_2SO_4$ as a precipitant in a 50 mM Tris/HCl buffer, pH 8.8. The crystals typically showed

Abbreviations used: CA, carbonic anhydrase; HCA, human CA.

[1] To whom correspondence should be addressed (e-mail debasish@cbse.uab.edu).

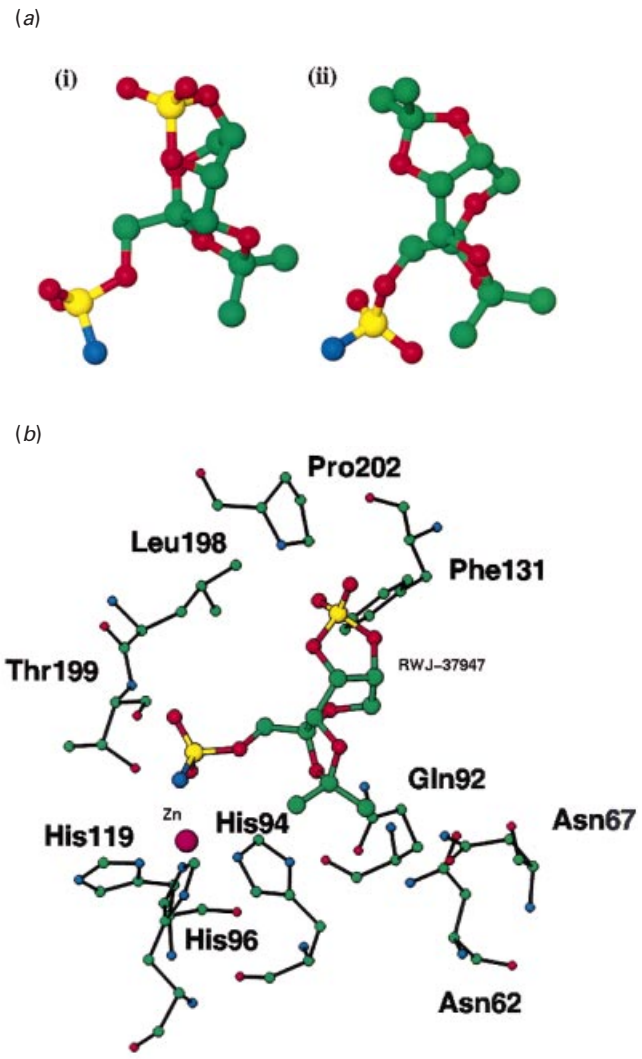

Figure 1 (a) Schematic drawings of (i) RWJ-37947 and (ii) topiramate and (b) a schematic representation of the interaction of RWJ-37947 with HCA II

(**a**) The RWJ-37947 adopts a skew conformation ($^3S_0$) for the tetrahydropyran ring in solution and in the solid state.

a flattened plate shape and belonged to the space group $P2_1$ with unit cell parameters of $a = 42.28$ Å, $b = 41.39$ Å, $c = 72.51$ Å and $\beta = 104.11°$.

Data collection

Diffraction data were collected at −170 °C on an R-AXIS IV imaging plate. A cryoprotectant solution was made by inclusion of glycerol, to 25 % (v/v), in the reservoir solution. Data were measured to a 2.1 Å resolution and processed using DENZO [10]. For all further computing the CCP4 suite [11] was used.

Structure solution and refinement

For structure solution we used an isomorphous HCA II structure reported previously (PDB code 1AM6 [12]). The initial model was refined by rigid-body minimization followed by simulated annealing and energy refinement, using CNS [13]. The ideal

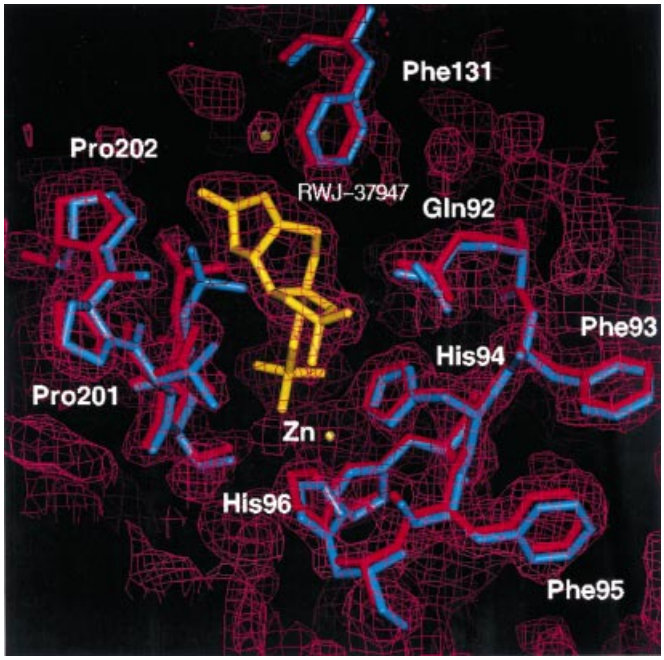

Figure 2 Representative section of the electron-density map (2Fo-Fc at 1.0 σ) showing the inhibitor RWJ-37947 in the active site

Superposition of the active-site residues in the absence of inhibitor (PDB code 2CBA) is shown by thin lines.

values of the parameters for the inhibitor model were taken from its X-ray structure, and the XPLO2D [13] dictionaries were used. Manual modelling of the HCA II–inhibitor complex was carried out with QUANTA. Crystallographic statistics for the structure are reported in Table 1.

RESULTS AND DISCUSSION

The structure of HCA II in the enzyme–inhibitor complex exhibited only minor differences in conformation when compared with that of the native protein [14]. There were two areas, corresponding to two external loops, residues 42–47 and 235–237, where the root mean square deviation was higher than the mean value for both structures, 0.32 Å. These two loops were not involved in any significant interaction. The first two residues at the N-terminus were disordered, although electron density for the backbone atoms was interpretable. The C-terminal region also presented some flexibility. Clear electron density was visible for the inhibitor (Figure 2).

The final model, including amino acid residues 3–261, one zinc ion, one molecule of the inhibitor and 194 water molecules, was refined to crystallographic R and R_{free} values of 0.18 and 0.23 respectively. The overall quality of the model is excellent, with all residues in the allowed regions of the Ramachandran plot. Figure 3 shows a ribbon [15] diagram of the crystal structure with the inhibitor molecule and the zinc ion.

The ionized nitrogen atom of the sulphamate group of RWJ-37947, which has a pK_a value of 8.51 [9], co-ordinates to zinc and displaces a hydroxide ion. In addition, this nitrogen atom donates a hydrogen bond to the hydroxy group of Thr-199. This hydroxy group also interacts with the Asp-106 OE1 (2.6 Å). One sulphamate oxygen (O_9) accepts a hydrogen bond from the backbone

Table 1 Crystallographic data for HCA II–RWJ-37947 interaction

Space group	$P2_1$
Cell dimensions	$a = 42.28$ Å, $b = 41.39$ Å, $c = 72.51$ Å, $\beta = 104.11°$
No. of reflections	169841
No. of unique reflections	16971
Percentage of reflections with $I > 3\ \sigma$	92.1%
Overall completeness (99–1.99 Å)	92.3%
Completeness of the data in the highest-resolution shell (1.86–1.8 Å)	77.2%
R_{merge}	7%
Overall I/σ	12.2
Refinement range	15–2.1 Å
Number of reflections	13549
R	0.018
R_{free}	0.023
R_{free} test set size	9.5%
Root mean square deviation from standard	
Bond lengths	0.01 Å
Bond angles	1.46°
Number of water molecules	178
Mean B value (all atoms)	12.2 Å^2

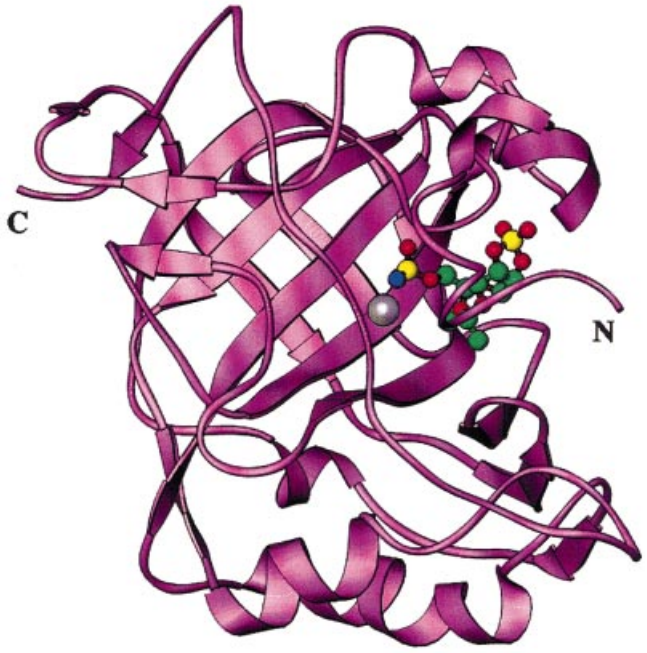

Figure 3 Ribbon diagram of the crystal structure with the inhibitor molecule and the zinc ion (centre)

Table 2 Interaction distances

(a) Zinc ion co-ordination. (b) Hydrogen-bond interactions between RWJ-37949 and HCA II. INH, inhibitor.

(a)

	Distance (Å)
His-96 Nϵ2	2.1
His-94 Nϵ2	2.0
His-119 Nϵ2	2.0
INH N-1	2.1
INH O-10	3.1

(b)

Protein	Inhibitor	Distance (Å)
Thr-199 Oγ	N-1	2.5
Thr-199 N	O-9	2.9
Gln-92 Nϵ2	O-3	3.2
Gln-92 Nϵ2	O-1	3.1
His-94 Nδ1	O-1	3.5
Pro-202 Cδ	O-7	3.3
Leu-198 Cδ1	O-6	3.5
Phe-131 Cζ	O-6	3.2
Phe-131 Cϵ2	O-6	3.5
Asn-67 Nδ2	C-8	3.1
Asn-67 Oδ1	C-8	3.4
Asn-62 Nδ2	C-8	3.4
His-94 Nϵ2	C-9	3.4

NH group of Thr-199, and interacts with Cα of Leu-198 (3.21 Å). The O_{10} atom is 3.1 Å away from the zinc ion. Besides co-ordination distances, angles and charges have to be taken into account in these enzyme–inhibitor complexes to evaluate the zinc ion co-ordination. The limits of this co-ordination angle should vary between 90° and 180°, for perfect bidentate binding and monodentate binding, respectively. The N_1–S–O_{10} bond angle is 77° (i.e. close to 90°). Therefore, although the co-ordination distance between Zn(II) and the sulphamate oxygen does not correspond strictly to inner-sphere co-ordination, taking into account the co-ordination angle and the charge, oxygen atom O_{10} could be considered as weakly co-ordinated to the zinc ion. The sulphamate would exhibit pseudo-bidentate co-ordination to zinc [16–18]. The other oxygen of the sulphamate group, O_8, has an intramolecular interaction with O_1 (2.7 Å, Figure 1b). The intermolecular interactions involving RWJ-37947 are shown in Figure 1(b), and Table 2 summarizes selected enzyme–inhibitor contacts.

The six-membered tetrahydropyran ring of RWJ-37947 adopts the skew conformation ($^3S_0$) in solution and in the solid phase [9]. This skew conformation is presumably favoured over the possible chair forms because of the two five-membered rings that are *cis*-fused on to the central pyranose ring (Figure 1a). Some compounds without the 4,5-ring favour a chair conformation and are virtually devoid of anti-convulsant activity [7]. It is interesting to note that the $^3S_0$ skew conformation of the pyran

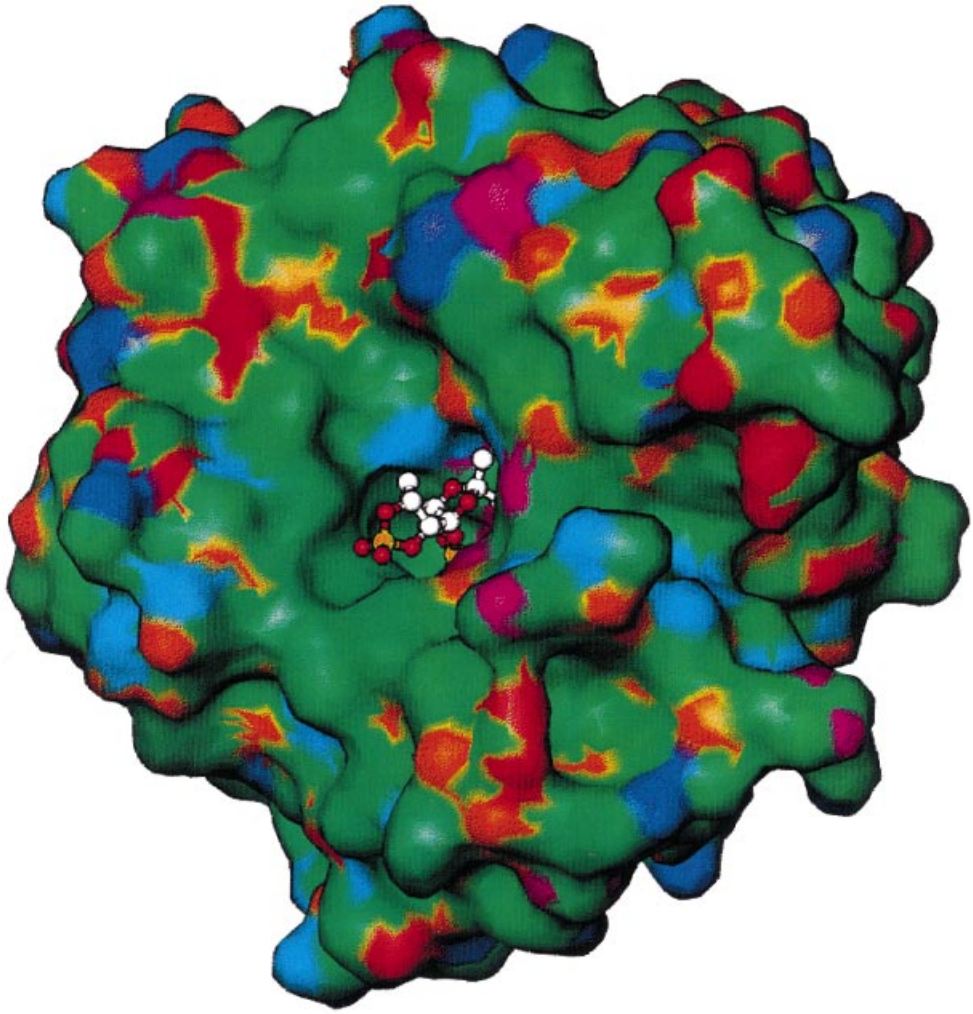

Figure 4 Molecular surface of HCA II–inhibitor complex

The surface is coloured on the basis of electrostatic potential: pink to orange, negative; purple, positive; green, neutral. The RWJ-37947 molecule is shown as a ball-and-stick model coloured by atom type. The sulphate group is positioned in the hydrophobic area of the active site.

ring is favoured here in the absence of crystal-packing forces and is central to complexation with HCA II (see below). The stereochemistry of the C-2 atom affects the binding conformation of the inhibitor as reflected by the orientation of the rings relative to the sulphamate group (Figure 1a). The stereochemistry and conformation cannot be accommodated easily in the CAII active site. The hydrophobic surface, comprising the side chains of Leu-198, Pro-201 and Pro-202, is exposed to solvent, and it is expected that inhibitors with benzyl or hydrophobic groups will shield these residues from water [19–21]. RWJ-37947 has a dioxolane ring with a tetrahedral carbon with two methyl substituents (2,3-isopropylidene group). However, steric factors prevent disposition of this group in the hydrophobic pocket because the cyclic sulphate group would then experience unfavourable steric interactions with Gln-92 and His-94.

RWJ-37947 is 30–100-fold more potent than topiramate as an inhibitor of CA [7]. Topiramate, a relatively weak inhibitor of erythrocyte CA in several species [7,9], differs structurally from RWJ-37947 by having a 4,5-isopropylidene group instead of a 4,5-cyclic sulphate group (Figure 1a). The increase in potency of RWJ-37947 is probably due to favourable interactions of the 4,5-cyclic sulphate, via its oxygen atoms, designated O-4, O-5, O-6 and O-7. The O-4 atom interacts with a water molecule while O-6 engages in a weak polar, dipole–quadrupole interaction [20] with the aromatic ring of Phe-131, and forms a weak hydrogen bond CH–O with Leu-198 [21]. The O-7 atom interacts with Pro-202 Cδ but O-5 does not participate in any intermolecular interaction. The oxygen of the pyranose ring (O-1), in addition to its intramolecular interaction with O-8, also makes a hydrogen bond with Nϵ2 of Gln-92 (Table 2). Finally, the isopropylidene ring of RWJ-37947 is situated on the polar area of the active site (Figure 4), and the methyl groups form hydrogen bonds [22] with the side-chain amide groups of Asn-67, Asn-62 and the His-94 Nϵ2 (Table 2). The electron density for His-64 is well defined and the residue is oriented towards the interior of the cavity pointing to the metal site, but it does not appear to interact with the inhibitor.

When we compare the active site of the present structure with that of HCA II without inhibitor, we notice no movement of the active-site residues. However, there are differences in the distribution of the water molecules in this region (Figure 4). The water molecules around His-64 are removed when the inhibitor is bound. However, new water molecules appear around the hydrophobic area of Leu-198, Pro-200 and Pro-202.

After oral and intravenous administration of RWJ-37947 to Sprague–Dawley rats at a dose level of 1 mg/kg, the blood concentrations were found to be elevated (> 3000 ng/ml) for a prolonged period of time (> 24 h), whereas the plasma concentrations were not (R. Shank and B. E. Maryanoff, unpublished work). Blood concentrations in dogs were also elevated at extended time points, e.g. > 2000 ng/ml at 144 h following an oral dose of 1 mg/kg, whereas plasma concentrations were quite reduced (< 20 ng/ml; R. Shank and B. E. Maryanoff, unpublished work). These data suggested the possibility of tight or irreversible binding of RWJ-37947 to erythrocytes, perhaps by the CA I and/or CA II present therein. Indeed, given the cyclic sulphate functionality in RWJ-37947 that can react with nucleophiles, it is conceivable that RWJ-37947 might alkylate CA at an active-site residue. Our crystallographic study reveals that RWJ-37947 remains intact when bound within the active site of HCA II and that no alkylation of any amino acid residue occurs.

The interactions of RWJ-37947 with HCA II are in good agreement with its IC_{50} value of 36 nM with the human erythrocyte enzyme. RWJ-37947 adopts a skew conformation ($^3S_0$) for the tetrahydropyran ring, which is favoured because of the two *cis*-fused five-membered rings on the central pyranose ring. This conformation may be important for its effective binding and its bioactivity. There was practically no movement of the residues in the active site of the structure of HCA II due to inhibitor binding. The ionized nitrogen of the inhibitor binds directly to the zinc ion, displacing the water molecule, and forms a hydrogen bond with Thr-199 Oγ. The cyclic sulphate group of RWJ-37947 forms a weak hydrogen bond with Pro-202 and Leu-198, and makes weakly polar interactions with Phe-131. These secondary interactions of the inhibitor can be improved by chemical modifications of the sulphate group, which will reduce the solvent-accessible surface and enhance the binding of the inhibitor in the active site. Significantly, the ligand was found to be intact in the complex, which serves to dispel any concern about RWJ-37947 irreversibly alkylating the enzyme through its 4,5-cyclic sulphate moiety.

We thank Professor Joseph Beckman and his colleagues for the protein used for crystallization. We also thank Dr Richard P. Shank for performing the enzyme kinetics studies. This work was supported by funds from the R. W. Johnson Pharmaceutical Research Institute, Spring House, PA, U.S.A.

Received 5 April 2001/8 August 2001; accepted 7 November 2001

REFERENCES

1 Lindskog, S., Henderson, L. E., Kannan, K. K., Liljas, A., Nyman, P. O. and Strandberg, B. (1971) Carbonic anhydrase. In The Enzymes, vol. 5 (Boyer, P. D., ed.), pp. 587–665, Academic Press, Orlando, FL
2 Pocker, Y. and Sarkanen, S. (1978) Carbonic anhydrase: structure, catalytic versatility, and inhibition. Adv. Enzymol. Related Areas Mol. Biol. **47**, 149–274
3 Maren, T. H. (1988) The kinetics of HCO_3-synthesis related to fluid secretion, pH controls and CO_2 elimination. Annu. Rev. Physiol. **50**, 695–717
4 Quigley, H. A. (1993) Pen angle glaucoma. N. Engl. J. Med. **328**, 1097–1106
5 Tielsch, J. M., Katz, J., Sommer, A., Quigley, H. A. and Javitt, J. C. (1994) Hypertension, perfusion pressure, and primary open-angle glaucoma. A population-based assessment. Arch. Ophthalmol. **112**, 69–73
6 Lindskog, S. (1997) Structure and mechanism of carbonic anhydrase. Pharmacol. Ther. **74**, 1–20
7 Maryanoff, B. E., Costanzo, M. J., Nortey, S. O., Greco, M. N., Shank, R. P., Shupsky, J. J., Ortegon, M. P. and Vaught, J. L. (1998) Structure-activity-studies on anticonvulsant sugar sulfamates related to topiramate. Enhanced potency with cyclic sulfate derivatives. J. Med. Chem. **41**, 1315–1343
8 Supran, C. T. and Scozzafava, A. (2000) Carbonic anhydrase inhibitors and their therapeutic potential. Exp. Opin. Therapeutic Patents **10**, 575–600
9 Dodgson, S. J., Shank, R. P. and Maryanoff, B. E. (2000) Topiramate as an inhibitor of carbonic anhydrase isosymes. Epilepsia. **41** (suppl. 1), S35–S39
10 Otwinowski, Z. and Minor, W. (1997) Processing of X-ray diffraction data collected in oscillation mode. Methods Enzymol. **276**, 307–325
11 Collaborative Computational Project, no. 4 (1994) The CCP4 Suite: programs for protein crystallography. Acta Crystallogr. **D50**, 760–763
12 Scolnick, L. R., Clements, A. M., Liao, J., Crenshaw, L., Hellberg, M., May, J., Dean, T. R. and Christianson, D. W. (1997) Novel binding mode of hydroxamate inhibitors to human carbonic anhydrase II. J. Am. Chem. Soc. **119**, 850–851
13 Brünger, A. T., Adams, P. D., Clore, G. M., Delano, W. L., Gros, P., Grosse-Kuntsleve, R. W., Jiang, J. S., Kuszewski, J., Nilges, M., Pannu, N. S. et al. (1998) Crystallography & NMR system: a new software suite for macromolecular structure determination. Acta Crystallogr. **D54**, 905–921
14 Hakansson, K., Carlsson, M., Svensson, L. A. and Liljas, A. (1992) Structure of native and apo carbonic anhydrase II and structure of some of its anion-ligand complexes. J. Mol. Biol. **277**, 1192–1204
15 Carson, M. (1997) Ribbons. Methods Enzymol. **277**, 493–505
16 Harding, H. H. (1999) The geometry of metal-ligand interactions relevant to proteins. Acta Crystallogr. **D55**, 1432–1443
17 Chakravarty, S. and Kannan, K. K. (1994) Drug-protein interactions. Refined structures of three sulfonamide drug complexes of human carbonic anhydrase I enzyme. J. Mol. Biol. **243**, 298–309
18 Christianson, D. W. (1991) Structural biology of zinc. Adv. Protein Chem. **42**, 281–355
19 Boricack-Sjodin, P. A., Zeitlin, S., Chen, H.-H., Crenshaw, L., Gross, S., Dantanarayana, A., Delgado, P., May, J. A., Dean, T. and Christianson, D. W. (1998) Structural analysis of inhibitor binding to human carbonic anhydrase II. Protein Sci. **7**, 2483–2489
20 Burley, S. K. and Petesko, G. A. (1988) Weakly polar interactions in proteins. Adv. Protein Chem. **39**, 125–189
21 Taylor, R. and Kennard, O. (1982) Crystallographic evidence for the existence of C-H...O, C-H...N and C-H...Cl hydrogen bonds. J. Am. Chem. Soc. **104**, 5063–5070
22 Jain, A., Whitesides, G. M., Alexander, B. S. and Christianson, D. W. (1994) Identification of two hydrophobic patches in the active-site cavity of human carbonic anhydrase II by solution-phase and solid-state studies and their use in the development of tight-binding inhibitors. J. Med. Chem. **37**, 2100–2105